Proceedings of the 21st ICSMGE, Vienna, Austria, 14 – 19 June 2026. Pistrol, Adam & Schweiger (eds.)
Published by: ÖGG, Austrian Society for Geomechanics, Salzburg, Austria, ISBN 978-3-9503898-4-5
https://doi.org/10.53243/ICSMGE2026-1404

Prediction of shaft resistance of bored piles in stiff high plasticity clay based on undrained shear strength

Jannie Knudsen, Jørgen S. Steenfelt, Helle Trankjær
7104 Geotechnical Disciplines, COWI, Denmark, jahs@cowi.com

Kenny K. Sørensen
Department of Civil and Architectural Engineering, Aarhus University, Denmark

ABSTRACT: This paper presents data on shaft resistance obtained from full-scale loading tests conducted on eight bored cast-in-place piles in Søvind marl, a very high plasticity clay. The focus is on examining the empirical adhesion coefficient, α, determined from the relationship between the unit shaft resistance, r_s, and the undrained shear strength, c_u. To enhance predictive accuracy, the results are integrated with a broader dataset from existing literature, encompassing fine-grained soils and stiff, high-plasticity clays such as London Clay and Danish Eocene Clay. A critical aspect of this study is the selection of a representative undrained shear strength, c_u, as it significantly affects the derived α coefficient. This issue is particularly pronounced in structured clays, such as Søvind Marl, which exhibit pronounced fissures and slicken-sided surfaces, leading to substantial variability between intact and fissured c_u measurements. The development of the empirical adhesion coefficient, α, with time is also considered, and results are recalibrated to a standard reference period of 30 days post-installation, ensuring that the concrete attains sufficient strength for reliable load testing. Despite considerable scatter in the data—attributable to variations in soil properties, pile geometry, installation methods, and test procedures—it is feasible to establish best-fit, lower-bound, and upper-bound envelopes for the α - c_u relationship. These envelopes are compared to the conservative guidelines in the Danish National Annex to Eurocode 7, Annex L, which are found to be overly conservative and not applicable to bored piles.

KEYWORDS: Bored piles, high-plasticity clay, shaft resistance, α - c_u relation, time effects.

1 INTRODUCTION

Accurate prediction of shaft resistance of bored cast-in-place piles is essential for safe and economical foundation design, especially in challenging soil conditions such as high-plasticity clays.

Traditional design approaches often rely on a conservative empirical adhesion coefficient, α, relating shaft resistance, r_s, to the soil's undrained shear strength, c_u. Initially, it was generally believed that the empirical adhesion coefficient, α, was primarily associated with the absolute value of the undrained shear strength, c_u, as illustrated by works such as Skempton (1959) and Kulhawy and Jackson (1989). However, further investigations revealed that the empirical adhesion coefficient, α, is intricately linked to the mean vertical effective stress throughout the pile depth (Goh et al., 2005, Chen et al., 2011). This demonstrates that the relationship between α and the soil's characteristics is more complex and involves factors beyond just the undrained shear strength.

This study aims to refine the understanding of the $\alpha - c_u$ relationship by analyzing full-scale loading tests in tension on eight instrumented bored piles installed in Søvind Marl at a test site in Hinge. Søvind Marl is a stiff, overconsolidated marine clay of very high plasticity found in Denmark, which presents unique geotechnical characteristics; including pronounced fissuring and complex mineralogy that complicate the assessment of pile-soil interaction.

By integrating the findings from the test site in Hinge with an extensive dataset from relevant literature - including soils such as London Clay (Skempton, 1959) and Danish Eocene Clay (Morrison et al. (2012) and unpublished work by Lyse et al. (2020)) - this research evaluates the influence of soil structure, residual stresses, and time-dependent strength gain on the empirical adhesion coefficient.

The extensive dataset that has been used also include data from two databases on pile loading tests that have been documented in the literature by Kulhawy and Phoon (1993), Chen and Kulhawy (1994) and Kulhawy and Chen (2003) as well as Chen et al. (2011). Limited information is available regarding the specific soil conditions; however, it is stated that the data is applicable to bored piles in fine-grained soils, most likely referring to clay with low or medium plasticity as classified by the Casagrande plasticity chart (Casagrande, 1932).

To establish a standardized relationship between the empirical adhesion coefficient, α, and the undrained shear strength, c_u, different representative undrained shear strength has been used - including the Danish field vane test and various triaxial compression tests. It is important to note that using triaxial compression tests implies that the empirical adhesion coefficient, α, will be significantly influenced by the presence of fissures (Skempton et al., 1969, Gasparre et al., 2007). As a result, it may not be directly comparable to an empirical adhesion coefficient, α, based on intact undisturbed undrained shear strength, $c_{u,intact}$, which can be determined through in-situ testing methods like the Danish field vane test.

Recognizing the critical significance of selecting a representative undrained shear strength, particularly in fissured clays, the paper also addresses the variability between intact and fissured strength measurements and their implications for design.

2 GROUND CONDITIONS AND TEST METHODS

2.1 *Ground conditions*

The test site in Hinge, Denmark, features predominantly Eocene clay known as Søvind Marl, a stiff, overconsolidated, and very high plasticity marine clay approximately 3 m below ground level. The marine Eocene clay lies beneath a clay till layer and exhibits glacial disturbances. The clay is identified as Søvind Marl mainly based on mineralogy and SEM analysis. An extensive geotechnical site investigation, including boreholes, field vane tests, CPTu, and laboratory tests on intact and remoulded samples, has been conducted to determine the soil's physical, chemical, and mechanical properties.

The determined classification properties of the Søvind Marl at the Hinge test site are given in Table 1. The clay's liquid limits exceed traditional classification limits, prompting use of

extended plasticity categories. Typically, the plasticity index is found to be inversely related to calcite content but appears more influenced by clay mineralogy at this site. The variable calcite content is reflective of historic climatic conditions and derives from coccoliths.

Table 1. Bulk unit weight, particle density, Atterberg limits and calcite content for Søvind Marl at the test site in Hinge.

Parameter	Symbol	Value (average)	Unit
Bulk unit weight	γ	16.0-17.4 (16.6)	kN/m^3
Particle density	ρ_s	2.77-2.78	g/cm^3
Water content	w_{nat}	46-62	%
Liquid limit	w_l	121-233	%
Plastic limit	w_{pl}	11-57	%
Plasticity index	I_p	84-203	%
Calcite content	-	4-36	%

At the Hinge test site, Søvind Marl exhibits relatively uniform soil conditions confirmed by CPTu soundings, showing net cone resistance (cf. Figure 1), friction ratio, and porewater pressure typical for heavily overconsolidated clays. Negative or near-zero pore pressures u_2 are generally measured behind the cone tip, which reflects the clay's stiff, overconsolidated nature.

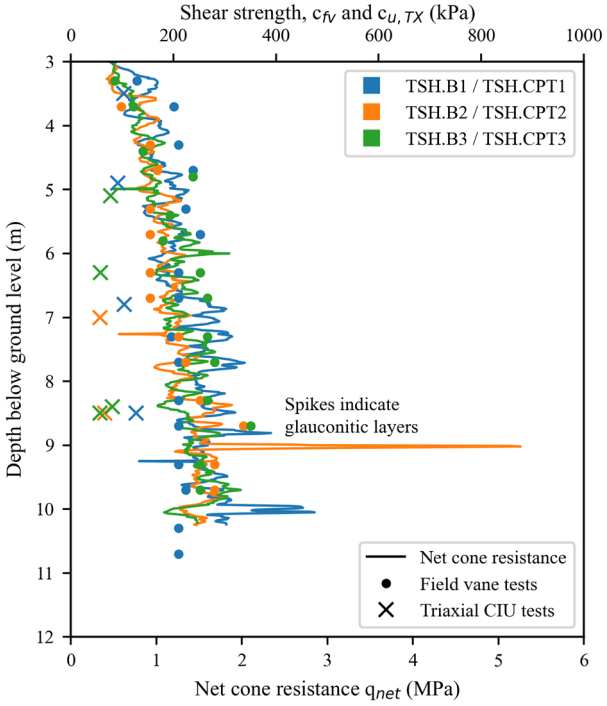

Figure 1. Measured field vane strength, c_{fv}, and undrained shear strength from isotropic consolidated undrained triaxial compression tests, $c_{u,TX}$, for borehole TSH.B1 – TSH.B3 and net cone resistance, q_{net}, from nearby CPTu soundings TSH.CPT1- TSH.CPT3.

Overall, Søvind Marl at the site is considered uniform for further analyses. The Søvind Marl at the Hinge test site has a measured field vane strength, c_{fv}, ranging from 100 to 300 kPa and an undrained shear strength from isotropic consolidated undrained triaxial compression tests, $c_{u,TX}$ from 60 to 130 kPa (cf. Figure 1).

The development of the site wide field vane strength, c_{fv}, with depth below ground level, z_d, can be estimated based on the following linear relationship:

$$c_{fv} = 96.7 + 17.1 \cdot z_d \quad (1)$$

Generally, a good correlation is observed between the field vane strength and cone tip resistance q_{net}, both show an, almost linear, increasing tendency with depth (except field vane strength result from BH 1, which indicate a constant strength with depth). The cone tip factor N_k, relating cone resistance to field vane strength, ranges around 5.2–6.2. The triaxial test results clearly show that fissuring reduces the undrained strength $c_{u,TX}$ compared to the field vane strength c_{fv}; a correlation factor μ averaging 0.36 relates the two. Due to the influence of fissuring and the small quantity of tests there is no clear tendency observed for $c_{u,TX}$ with depth.

Groundwater levels at the Hinge test site were measured in filters placed both within the Søvind Marl (8-10 m depth) and the overlying soils (1.5-3.5 m depth). The measured groundwater levels vary from 3 m below ground level to ground level. Water levels fluctuated by about 1 m annually, peaking in early spring and dipping in autumn.

Prior to installation of the bored piles, the top 3.4 m of soil was predrilled (Ø1000 mm diameter) and replaced by sand (poorly graded medium sand) at each pile location. This was done to minimize contributions from the upper soil layers to the shaft resistance and thereby making it easier to deduce contributions from the underlying layers of marine Eocene clay. The replacement with sand is assessed not to have any influence on the marine Eocene clay, as it has a very low permeability. The performance of the shaft resistance on the bored piles in the sand layers are discussed in section 3.4.

2.2 *Test piles and pile instrumentation*

The test piles, designed to prevent tensile loads exceeding structural strength, are 9 m long (0.62 m diameter) with 0.5 m above ground, made of A35 MPa concrete and reinforced with eight Y32 bars and shear reinforcement. Two Ø63.5 mm GEWI PLUS bars were installed to 6.5 m depth to transfer tensile loads from hydraulic jacks to the reinforcement.

Figure 2 shows details of the pile instrumentation. Instrumentation includes tell-tales and strain gauges at multiple levels to measure displacements and strains caused by load, enabling estimation of shaft resistance distribution. Tell-tales and strain gauges were positioned near the pile base and clay-sand interface to measure displacements and strains within the test piles originating from the sand and clay layer, respectively. Additional strain gauges were located at ground level and in the middle of the sand and clay layer to refine strain data along the length of the test piles. Finally, three cables with distributed fibre optic sensors along the pile length measure highly detailed strain and temperature along the entire length of the test piles.

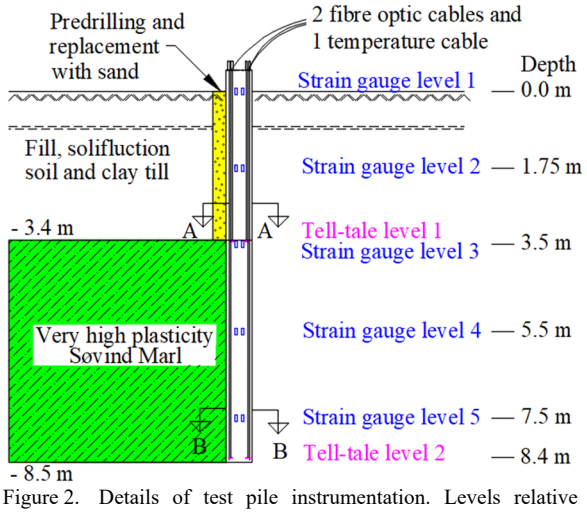

Figure 2. Details of test pile instrumentation. Levels relative to ground level.

Monitoring equipment is installed in pairs on opposite sides of the neutral axis to separate bending moments, caused by eccentric loading on test piles, from axial loads, see Figure 3.

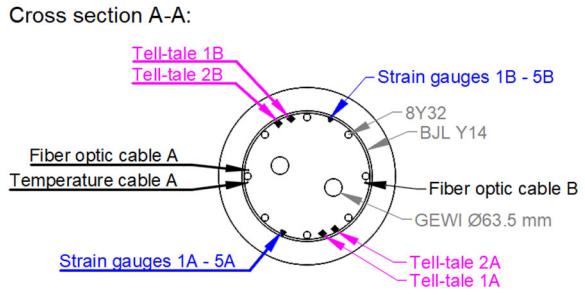

Figure 3. Upper cross section A-A.

2.3 *Pile load tests and test setup*

Eight instrumented bored piles were installed in August 2019 using a Bauer drilling rig (BG 36 H) that provides Kelly drilling. The casing was lowered simultaneous with the drilling equipment and kept at a depth that allowed drilling inside the casing. An auger was used for drilling inside the casing and a bucket was used to clean the bottom of the borehole before concreting. No water was used in the borehole during drilling and cleaning. The casing was always kept 1 m above ground to ensure against contamination by debris, and the reinforcement cage was lowered into the borehole before concreting.

Testing of the first test piles commenced 1.5 months after installation to allow for concrete curing. Subsequent piles were tested after 7 months and ~3 years to study set-up effects on shaft resistance. The full-scale test program was carried out as static tensile load tests. A steel traverse system with cribbing and load distribution beams was assembled around each test pile to support static tensile loading, see Figure 4. The loading system comprised four hydraulic jacks (each 300-ton capacity), connected to the piles via GEWI PLUS bars to transfer forces.

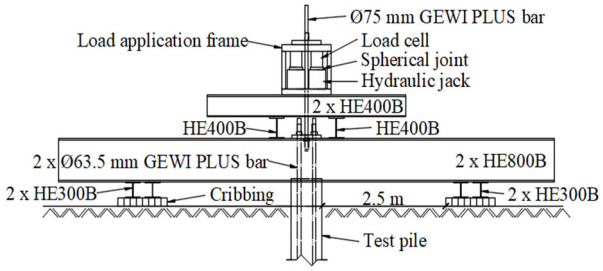

Figure 4. Sketch of steel traverse system for static tensile load tests.

Two loading procedures were used: Maintained Load (ML) test and Constant Rate of Uplift (CRU) test.

In the ML test, the tensile load was applied incrementally, where loads were adjusted smoothly over ~3 minutes to avoid shocks. The CRU test started like the ML test, then switched to a constant uplift rate once failure was imminent, see Table 2.

3 RESULTS

3.1 *Mobilized pile capacities and shaft resistance*

Shaft resistance, R_s, of the test piles, determined from static tensile load tests, corresponds to their total bearing capacity based on load-displacement curves. The load-displacement curves are based on data from the displacement transducers on pile top, and no corrections are made relative to the surveyor's level. Table 3 gives an overview of the performed pile load test including obtained total shaft resistance, R_s, and displacement at failure, d_f.

Table 2. Overview of loading procedures.

Test type	Phase	Condition	Step (kN)	No. (-)	Time (min)	Rate (mm/h)
ML	1	Loading	100	5	≥ 30	-
		Unloading	100	5	5	-
		Break	0	1	30	-
	2	Loading	125	5/6	≥ 30	-
		Near failure	50	4/0	≥ 30	-
CRU	1	Loading	100	2	≥ 30	-
		Unloading	100	2	5	-
		Break	0	1	30	-
	2	Loading	100	6	≥ 30	-
		Near failure	50	4	≥ 30	-
		Imminent failure	-	-	-	20

Table 3. Overview of pile test and results.

Test pile no.	Test type	Age (month)	R_s (kN)	d_f (mm)	E_tA (GN)
1	ML	1.5	824	8.9	12.5
7			748	3.6	14.0
3	CRU	7	884	9.1	14.3
5			881	11.6	14.1
8			913	8.1	15.0
2	CRU	34	837	10.5	16.1
4			909	8.3	16.1
6			955	7.9	15.4

3.2 *Determination of axial pile stiffness*

The axial stiffness is determined by directly analyzing the test records, using the tangent stiffness method as proposed by Fellenius (1989). The axial stiffness, not the applied load, typically exhibits a linear relationship to the imposed strains, $\varepsilon_{t,a}$. In this method, the Young's modulus of the test piles is assumed to be equal to the secant modulus.

The tangent stiffness method establishes a relationship between the tangent modulus (or tangent axial stiffness) derived from the stress-strain (or load-strain) curve and the secant modulus (or secant axial stiffness). The determined axial pile stiffness, E_tA, was generally constant within low strain ranges (0-60 με), ranging approximately from 12.5 to 16.1 GN across piles, see Table 3.

In addition, the direct secant method is also employed to determine the axial stiffness, but it is applicable only to strain gauges positioned either above or immediately below the ground level, as outlined by Fellenius (2023). The tangent and secant methods provided compatible stiffness estimates, capturing the pile's elastic response under tensile loading.

3.3 *Load distribution in test piles*

Load distribution along the test piles is determined as strain measurements multiplied by the previously calculated axial stiffness, adjusted for reduced stiffness near the pile base due to the absence of GEWI bars. Variations in axial stiffness can occur along the pile length due to curing, temperature, and soil conditions, though detailed analysis was beyond the project scope.

Strains were averaged for each load step and corrected for thermal effects. Most piles showed tensile strains highest near the ground level, decreasing with depth, indicating tension along the piles. For the top strain gauge level, applied load was used directly due to boundary effects and limited load transfer capacity near the pile top. An example of a load distribution profile is given for test pile 8 in Figure 5.

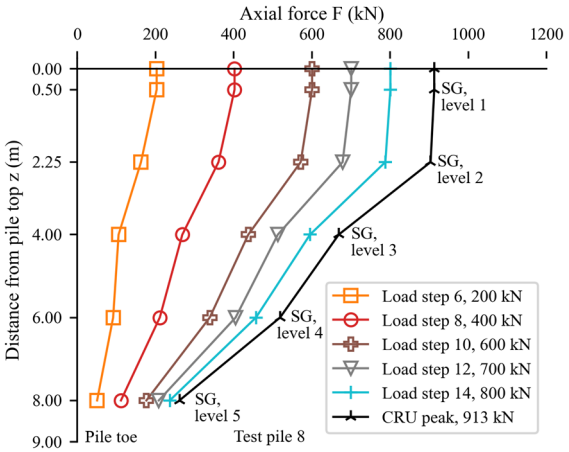

Figure 5. Back-calculated axial force along the length of test pile 8 for every other load step in Phase 2. Phase 1 is not shown.

Load distribution profiles from the maintained load (ML) tests showed generally a linear and consistent mobilization of shaft resistance below strain gauge level 2. In constant rate of uplift (CRU) tests, load distribution indicated low shaft resistance in the upper sand layer and higher resistance deeper in the lower sand layer and the clay layers, with variations among test piles.

3.4 *Unit shaft resistance*

The mobilized unit shaft resistance, r_s, was calculated between each strain gauge level as the difference between the back-calculated axial forces divided by the shaft area. These values are then plotted against the vertical displacement between the pile and soil, $\delta_{pile,soil}$, where the vertical displacement between the pile and soil is determined by subtracting the elastic lengthening, $\delta_{pile,e}$, between two adjacent strain gauges from the corresponding vertical displacement at the pile top, δ.

Empirical functions were fitted to the data for the sand and clay layers in order to establish coherent mobilization curves. The Zhang function (Zhang and Zhang, 2012) is selected for the sand layers, while the Vijayvergiya function (Vijayvergiya, 1977) is selected for the clay layers.

The upper and lower clay layers had average shaft resistances of 53 kPa and 68 kPa respectively, with notable variations between piles, see Table 4. Shaft resistance increased about 28% from upper to lower clay layers, slightly above expectations from field vane strength increases (20%). An example of mobilized unit shaft resistance is given for test pile 8 in Figure 6.

The upper sand layer showed low resistance (average ~12 kPa), while the lower sand layer surprisingly had much higher values (average ~50 kPa), suggesting significant residual stresses were developed and affected the pile behavior despite uniform sand replacement.

These surprisingly high ultimate values of mobilized unit shaft resistance in the sand layers indicate that a modified test pile setup should have been chosen. In hindsight, a solution with double casing above the marine Eocene clay layer, leaving air in between the two, would have been preferable despite sacrificing the casings.

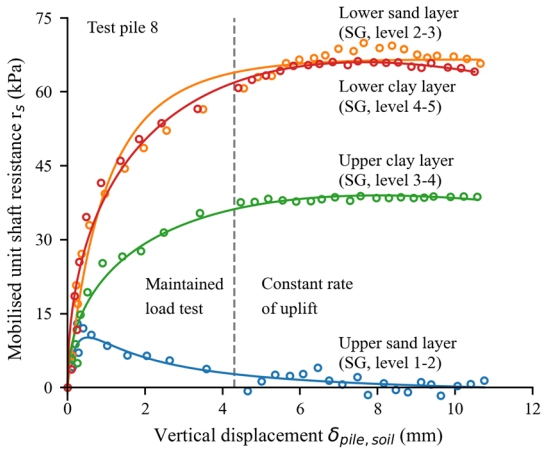

Figure 6. Mobilized unit shaft resistance for test pile 8.

3.5 *Correction for residual stresses*

During static pile loading tests conducted in tension, the resistive force, R_b, at the pile base can either be zero or reach the maximum suction force ($A_b \cdot 1\ atm \sim 31$kN) during failure. To determine whether the axial force at the pile base is zero or equal to the maximum suction force, the load distribution along the length of the test piles is investigated during failure. An example is given for test pile 8 in Figure 7.

However, extending the load distribution lines to the pile base did not reach expected zero or maximum suction values, implying residual stresses affect pile behavior during loading.

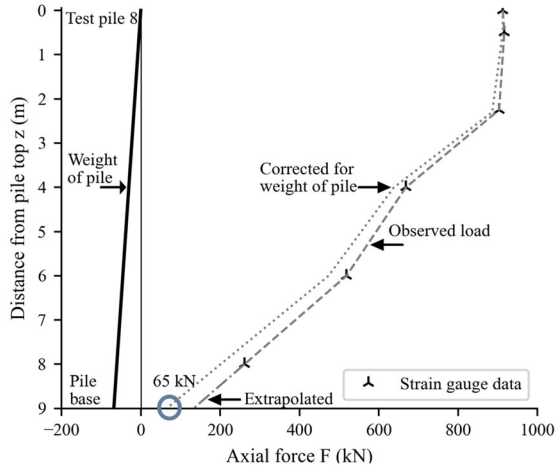

Figure 7. Axial load distribution along the length of test pile 8 based on vibrating wire strain gauge (VWSG) data, which corrected for weight of the test pile has 65 kN in tension at pile base.

The mobilized unit shaft resistance, r_s, was recalculated considering residual stresses after a new method for interpretation of residual stresses (Knudsen, 2024).

Table 4 gives an overview of the mobilized shaft resistance in Søvind Marl, r_s, and displacement at failure, d_f, as well as the correction needed to account for residual stresses, Δr and the corresponding empirical adhesion coefficient, α_{cfv}.

4 ANALYSIS OF FIELD TEST RESULTS

4.1 *Representative undrained shear strength, c_u*

The mobilized unit shaft resistance, r_s, relates to the undrained shear strength, c_u, via an empirical adhesion coefficient, α:

$$r_s = \alpha \cdot c_u \quad (2)$$

Table 4. Mobilized shaft resistance in Søvind Marl.

Test pile no.	Age (month)	Layer	r_s (kPa)	d_f (mm)	Δr_r (kPa)	α_{cfv} (-)
7	1.5	Upper	57	3.3	-9	0.28
		Lower	47	3.3	19	0.32
3	7	Upper	65	14.4	1	0.38
		Lower	70	11.6	2	0.35
5		Upper	57	11.9	3	0.34
		Lower	75	11.8	-11	0.31
8		Upper	39	7.6	12	0.29
		Lower	66	7.5	8	0.36
2	34	Upper	58	10.3	-3	0.32
		Lower	73	10.3	-3	0.34
4		Upper	51	8.7	5	0.32
		Lower	85	7.4	-2	0.40
6		Upper	48	8.6	11	0.34
		Lower	80	8.5	-5	0.36

Selecting a reference c_u is crucial, especially for fissured, slicken-sided clays like Søvind Marl. Two main tests provide undrained shear strength, c_u: the Danish field vane test (giving intact shear strength, $c_{u,intact}$) and isotropic consolidated undrained triaxial compression (CIU) test (reflecting lower fissured strength, $c_{u,fissured}$, due to failure along fissures).

The field vane test is widely used in Denmark for its reliability, cost-effectiveness, and the measured shear strength is independence from fissuring. However, it does not provide information about potential disturbance caused by pile installation in the surrounding soil, including horizontal or vertical soil movements. It also does not account for generation of excess porewater pressure or stress changes resulting from the curing process of bored piles, which can affect both normal and shear stresses at the soil-pile interface.

The CIU test is more complex and sensitive to specimen fissuring and sampling disturbance, which reduces the measured shear strength, but it can assess soil behavior under different states. This testing method is relatively expensive and time-consuming to perform and often yields inconsistent results due to variations among individual test specimens. Based on (Knudsen, 2024) and Grønbech (2015), the fissured undrained shear strength, c_u^{CIU} of Søvind Marl, from isotropic consolidated undrained triaxial compression (CIU) test is found to range between approx. 20% and 80% of the field vane strength, c_{fv}, obtained from the Danish field vane test. This variation depends on the degree of fissuring present in the specimen.

Furthermore, it could potentially provide a more comprehensive understanding of the soil's behavior and allow for consideration of the installation disturbances and the curing effects on the surrounding soils from the bored pile. These considerations can be studied by testing specimens in different states like e.g. a remolded, reconstituted, or fully softened state.

In Danish practice, the intact shear strength from the field vane test is preferred for predicting the ultimate shaft resistance of bored piles since mobilization of the ultimate shaft resistance involves large soil volumes and forced failure plane along the pile shaft. Fissured strength is more relevant for base failure.

Overall, the undrained shear strength, $c_{u,intact}$, from the field vane test is the recommended reference for design, enabling consistent determination of the adhesion coefficient, α.

4.2 *Derived α coefficient and development with time*

The empirical adhesion coefficient, α, for test piles 2-8 was determined using undrained shear strength, c_u, from field vane tests at depths of 4.5 m and 6.5 m for the upper and lower clay layers, respectively, see Table 4. The observed α values ranged from 0.28 to 0.38 (upper layer) and 0.31 to 0.40 (lower layer), significantly higher (about 2.3 to 3.3 times) than the Danish code value of 0.12 for bored piles. Variability in α may result from residual stress adjustments, clay structure degradation during installation, and shaft resistance development over time.

The α coefficient slightly increases over time following a logarithmic trend, gaining approx. 0.03 per decade after pile installation, though with considerable scatter, see Figure 8.

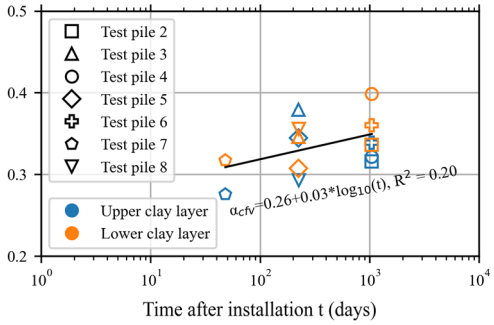

Figure 8. Development of empirical adhesion coefficients, α_{cfv}, with time for Søvind Marl determined for test piles 2-8, categorized into the upper clay layer (strain gauge level 3-4) and the lower clay layer (strain gauge level 4-5).

The empirical adhesion coefficients, α_{cfv}, obtained are recalibrated to represent a period of one month (30 days) after the installation of the piles. The recalibration is performed using the log linear relationship presented below:

$$\alpha_{cfv} = 0.26 + 0.03 \cdot \log_{10}(t) \quad (3)$$

4.3 *Best fit, lower bound and upper bound envelopes for the α-c_u relation*

A best-fit, lower bound, and upper bound envelope for the empirical adhesion coefficient, α, versus intact undrained shear strength, $c_{u,intact}$, relation is developed based on the results from test site Hinge and an extensive dataset from relevant literature cf. section 1. In the Skempton study (1969), 17 out of the 34 pile loading tests conducted on bored piles, were actually micropiles with a pile diameter smaller than 300 mm or nearly micropiles, characterized by pile diameters of either 305 or 356 mm. These micropiles are excluded as they do not represent typical scenarios encountered in normal construction practice for bored piles.

For fine-grained soils, a power-law fit captures the data, with envelopes representing the 5th and 95th percentiles.

Best fit:

$$\alpha_{intact} = 6.65 * c_{u,intact}^{-0.59} \quad (4)$$

Upper bound (95th percentile):

$$\alpha_{intact} = 8.12 * c_{u,intact}^{-0.56} \quad (5)$$

Lower bound (5th percentile):

$$\alpha_{intact} = 4.04 * c_{u,intact}^{-0.57} \quad (6)$$

Here, α_{intact} is the empirical adhesion coefficient and $c_{u,intact}$ is the intact undrained shear strength or the equivalent intact undrained shear strength for fissured clays.

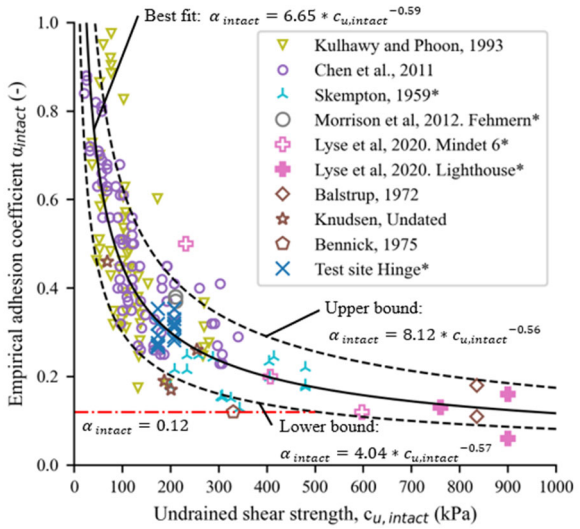

Figure 9. Relation between empirical adhesion coefficients, α_{intact}, and the intact undrained shear strength, $c_{u,intact}$, for fine-grained soils, characterized by best fit, lower bound and upper bound envelopes for the α-c_u relation. High plasticity clays are marked with * in the legend.

The lower bound envelope of the empirical adhesion coefficient α notably exceeds the Danish National Annex (DS/EN_1991-1-5_DK_NA, 2012) value of 0.12. It is 2.4 times higher at an undrained shear strength of 100 kPa and 1.6 times higher at 200 kPa. This Danish specification (red dashed-dot line in Figure 9) applies to strengths up to 500 kPa.

5 CONCLUSIONS

This study provides valuable insights into the shaft resistance behavior of bored cast-in-place piles installed in Søvind Marl, a highly plastic, fissured marine clay with complex soil structure. Full-scale static tensile load tests on eight instrumented piles revealed that the empirical adhesion coefficient, α, relating unit shaft resistance to the undrained shear strength, c_u, is significantly higher than the conservative value recommended in the Danish National Annex to Eurocode 7. This discrepancy highlights the limitations of existing design provisions for bored piles in high-plasticity clays.

This research draws attention to the importance of critical evaluation of the representative undrained shear strength to be used for design, emphasizing the importance of selecting intact shear strength measured from field vane tests, especially for fissured, slicken-sided clays, over fissured strength from triaxial tests. Furthermore, the study demonstrates that shaft resistance, and thus α, evolves over time.

By integrating the test results from test site Hinge with an extensive database from fine grained soils cf. section 1, including high plasticity clay (London Clay and Danish Eocene Clay), best-fit, lower bound, and upper bound envelopes for the empirical adhesion coefficient, α, versus intact undrained shear strength, $c_{u,intact}$, relation have been developed. These envelopes account for variability in soil properties, pile geometry, installation techniques, and test methodologies and provide a more reliable framework for pile capacity prediction.

Overall, the findings challenge current conservative guidelines and suggest that more realistic α values can lead to optimized foundation designs. Future work may focus on refining the understanding of soil-pile interaction mechanisms in fissured clays and expanding the dataset to other soil types for broader applicability.

6 ACKNOWLEDGEMENTS

The authors would like to thank COWI, COWIfonden and Innovation Fund Denmark for providing funding for this study. Furthermore, Par Aarsleff A/S for geotechnical investigations and installation of the instrumented test piles, DMT Gründungstechnik, GmbH, for pile loading test and Saint-Gobain Weber A/S for access to the test site.

7 REFERENCES

CASAGRANDE, A. 1932. Research on the Atterberg Limits of soils. Public Roads.

CHEN, Y.-J., LIN, S.-S., CHANG, H.-W. & MARCOS, M. C. 2011. Evaluation of side resistance capacity for drilled shafts. *Journal of marine science and technology,* 19.

CHEN, Y. & KULHAWY, F. 1994. Case history evaluation of the behavior of drilled shafts under axial and lateral loading.: Electric Power Research Inst., Palo Alto, CA (United States); Cornell Univ., Ithaca, NY (United States). Geotechnical Engineering Group.

DS/EN_1991-1-5_DK_NA 2012. National Annex to Eurocode 1: Actions on structures - Part 1-5: General actions - Thermal actions. Danish Standard.

FELLENIUS, B. 2023. *Basics of foundation design*, www.Fellenius.net.

FELLENIUS, B. H. 1989. Tangent modulus of piles determined from strain data. *In:* KULHAWY, F. H. (ed.) *The American Society of Civil Engineers, ASCE, Geotechnical Engineering Division, 1989 Foundation Congress.*

GASPARRE, A., NISHIMURA, S., COOP, M. R. & JARDINE, R. J. 2007. The influence of structure on the behaviour of London Clay. *Géotechnique,* 57**,** 19-31.

GOH, A. T., KULHAWY, F. H. & CHUA, C. 2005. Bayesian neural network analysis of undrained side resistance of drilled shafts. *Journal of Geotechnical and Geoenvironmental Engineering,* 131**,** 84-93.

GRØNBECH, G. L. 2015. *Søvind Marl - Behaviour of a plastic fissured Eucene clay.* PhD PhD thesis, Aalborg University.

KNUDSEN, J. 2024. *Soil-pile interaction for bored cast-in-situ piles in stiff clays.* PhD, Aarhus University.

KULHAWY, F. & CHEN, Y. 2003. Evaluation of undrained side and tip resistances for drilled shafts. *In:* CULLIGAN, P. J., EINSTEIN, H. H. & WHITTLE, A. J. (eds.) *Soil and Rock America 2003: 12th Panamerican Conference on Soil Mechanics and Geotechnical Engineering.* Cambridge, Massachusetts, USA.

KULHAWY, F. H. & JACKSON, C. S. Some observations on undrained side resistance of drilled shafts. Foundation Engineering: Current principles and practices, 1989. ASCE, 1011-1025.

KULHAWY, F. H. & PHOON, K.-K. Drilled shaft side resistance in clay soil to rock. Design and performance of deep foundations: Piles and piers in soil and soft rock, 1993. ASCE, 172-183.

LYSE, C., CHRISTOFFERSEN, A. G. & CHRISTENSEN, R. 2020. A reflection on the capacity and service responce of large diameter cast-in-place bored piles installed in fissured and highly plastic Eocene clay at the port of Aarhus, Denmark. Unpublished: Rambøll.

MORRISON, P., HAMMAMI, R., HANSEN, G. L. & BAILIE, P. Fehmarnbelt Fixed Link- Installation and testing of driven steel tube piles and bored cast-in-place concrete piles. Nordic Geotechnical Meeting 2012, 2012 Copenhagen, Denmark. dgf-Bulletin 27, 507-514.

SKEMPTON, A. W. 1959. Cast in-situ bored piles in london clay. *Geotechnique,* 9**,** 153-173.

SKEMPTON, A. W., SCHUSTER, R. L. & PETLEY, D. J. 1969. Joints and Fissures in the London Clay at Wraysbury and Edgware. *Géotechnique,* 19**,** 205-217.

VIJAYVERGIYA, V. N. Load-movement characteristics of piles. 4th Annual Symposium of Waterway, Port, Coastal and Occean Division of ASCE, 9-11 March 1977 1977 Long Beach, California. ASCE, 269-284.

ZHANG, Q.-Q. & ZHANG, Z.-M. 2012. A simplified nonlinear approach for single pile settlement analysis. *Canadian Geotechnical Journal,* 49**,** 1256-1266.